Electronic Supplementary Information

Large-scale 2D PbI$_2$ monolayers: experimental realization and its indirect band-gap related properties

Mianzeng Zhong,[‡a] Shuai Zhang,[‡b,c] Le Huang,[a] Jingbi You,[a] Zhongming Wei,[*a] Xinfeng Liu,[*b] and Jingbo Li[*a]

[a.] *Institute of Semiconductors, Chinese Academy of Sciences, P.O. Box 912, Beijing 100083, China, E-mail: zmwei@semi.ac.cn; jbli@semi.ac.cn*

[b.] *CAS Center for Excellence in Nanoscience, CAS Key Laboratory of Standardization and Measurement for Nanotechnology, National Center for Nanoscience and Technology, Beijing 100190, China. E-mail: liuxf@nanoctr.cn*

[c.] *School of Physics and Electronics, Shandong Normal University, Jinan 250014, China*

‡ These authors contributed equally to this work.

Experimental section

Synthesis of monolayer and few-layer PbI$_2$.

The monolayer and few-layer PbI$_2$ were grown on SiO$_2$/Si substrate by a catalyst-free PVD process in a horizontal vacuum tube furnace. In a typical synthesis, 0.1 g PbI$_2$ power was added to a ceramic boat as the source material and placed at the center of the furnace. Argon (Ar) is selected as the carrier gas. The substrate was placed on top of the ceramic boat (see Fig. S1a). The temperature rose from 303 K to 683 K at a rate of 24 K/min, and the temperature was kept at 683 K for 1 min, 2 min, and 3 min. Then the furnace was cooled down to room temperature quickly. Meanwhile, increasing the gas flow rate of Ar rapidly expel the vapour with PbI$_2$ molecules in a remarkably short period of time. The growth temperature of PbI$_2$ as a function of the growth time is shown in Fig. S1b.

Fabrication of photodetectors.

The monolayer and few-layer PbI$_2$ based photodetectors fabricated on the SiO$_2$/Si substrate (Si substrate with 300 nm SiO$_2$ insulating top layer) by a "nanowire mask moving" technique. One nanowire (about 200 nm) serving as the mask was fixed tightly on the top surface of PbI$_2$ crystals, and then a pair of Au electrodes was deposited onto the substrate by thermal evaporation. Finally, by slightly removing the nanowire mask, the Au electrodes were fabricated and a gap was produced between the two electrodes.

Measurement and Characterization.

The phase compositions, crystallographic structures, morphologies of the as-prepared materials were examined by X-ray diffraction (XRD) technique with Cu Ka irradiation, optical microscope, and high-resolution transmission electron microscopy (HRTEM; JEM-2100F, JEOL). Raman spectra were measured by the 532 and 633 nm laser. Photoluminescence spectra were measured using a laser with a 405 nm wavelength. Current-voltage (I-V) characteristics of the device were recorded with transistor test system (Agilent-B2902). The spectral response was obtained by using a 450 nm laser.

Density Functional Theory Calculations.

The calculations are performed by using the projector augmented plane-wave (PAW) method[1,2] within the framework of DFT in the Vienna ab initio Simulation Package (VASP).[3] The generalized gradient approximation (GGA) of Perdew, Burke, and Ernzerhof (PBE) functional[4] is adopted for electron exchange and correlation. The vdW interlayer interaction is described by opt PBE-vdW.[5] The spin–orbit coupling effect is also considered in the calculation. The Ceperly–Alder functional form of the local density approximation (LDA)[6] and the Heyd–Scuseria–Ernzerhof (HSE06) hybrid functional[7] are also adopted for the calculations of PbI_2 electronic structures. A vacuum larger than 15 Å is used to eliminate the interaction between adjacent images. The cut off energy for the plane-wave basis set is set to 500 eV.[8] In the total energy calculations of PbI_2 layers, a set of ($15 \times 15 \times 1$) k-point samplings was used for Brillouin zone integration.[9] All of the structures are fully relaxed with a force tolerance of 0.01 eV/Å. For the calculations of the surface energy, the "slab" approach is used. The relaxed supercells used to construct the surface models are shown in Fig. 2. For each face, 15 atomics (5 Pb atomics and 10 I atomics) are used in the slab. The surface energy (E_{surf}) is calculated as: $E_{surf}=(E_{slab}-nE_{bulk})\cdot(2A)^{-1}$, where E_{slab} refers to the total energy of the slab, E_{bulk} is the energy for bulk PbI2 per unit cell, n is the number of bulk unit cells in the slab, and A is the surface area.[10]
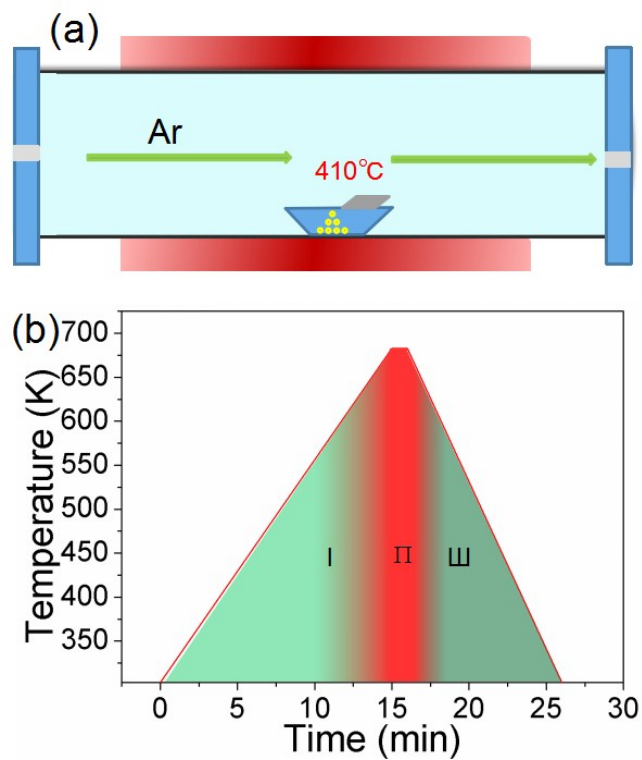
Fig. S1 (a) Schematic diagram of experimental setup used for the synthesis of PbI$_2$ crystals. (b) The growth temperature of PbI$_2$ as a function of the growth time.
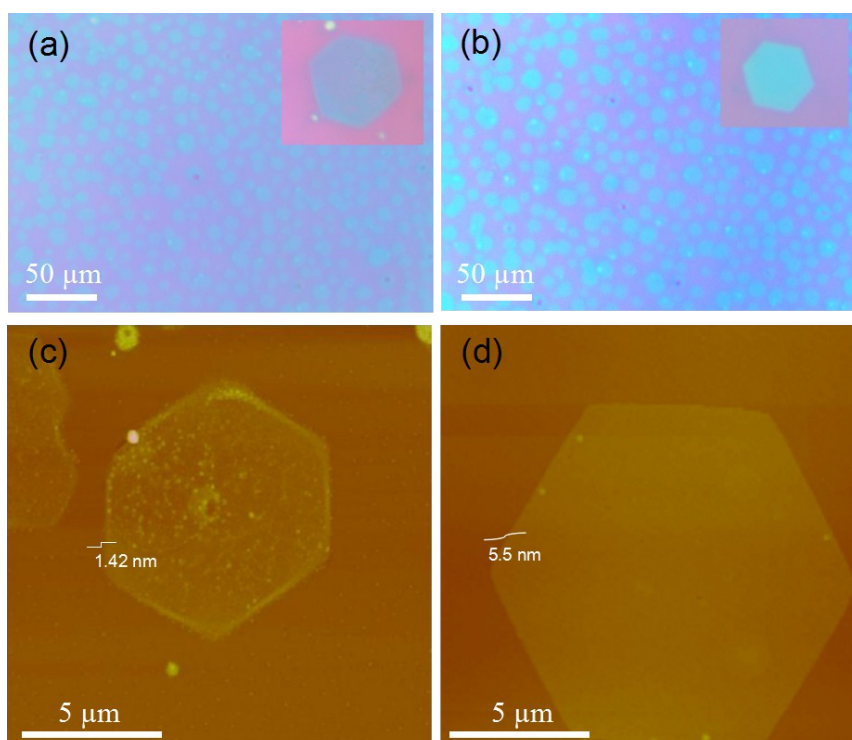

Fig. S2 (a) Optical and (c) AFM images of as-prepared PbI$_2$ microsheets with growth time of 2 min; (b) Optical and (d) AFM images of as-prepared PbI$_2$ microsheets with growth time of 3 min.
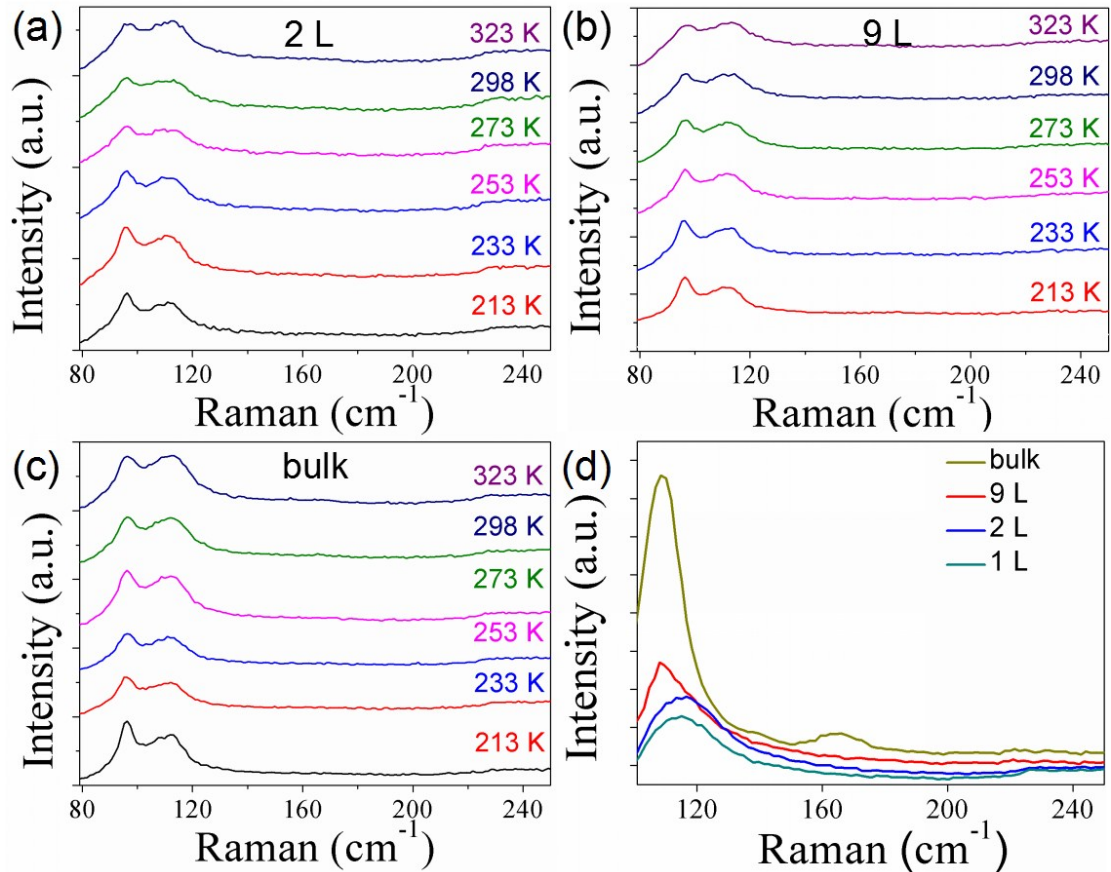
Fig. S3 (a), (b) and (c) Raman spectra of bilayer, 9-layer and bulk PbI_2 recorded at different temperatures, respectively. The excitation light source is a 633 nm laser. (d) Room-temperature Raman spectra of PbI_2 samples with different thicknesses excited by a 532 nm laser.
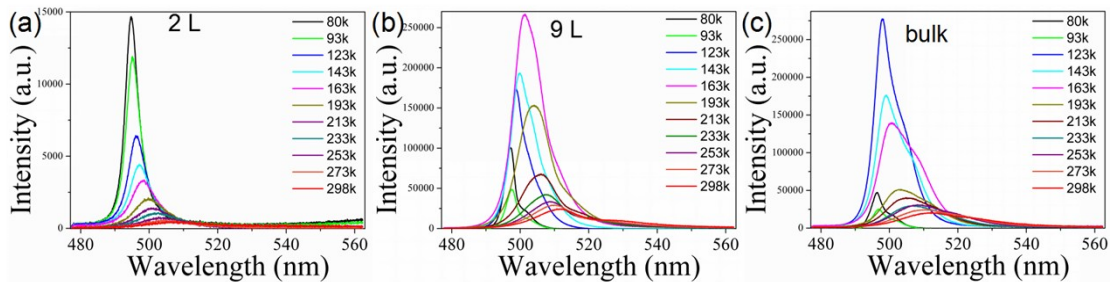

Fig. S4 Photoluminescence spectra of (a) bilayer, (b) 9-layer and (c) bulk PbI_2 recorded at different temperatures, respectively. The excitation light source is a 405 nm laser.
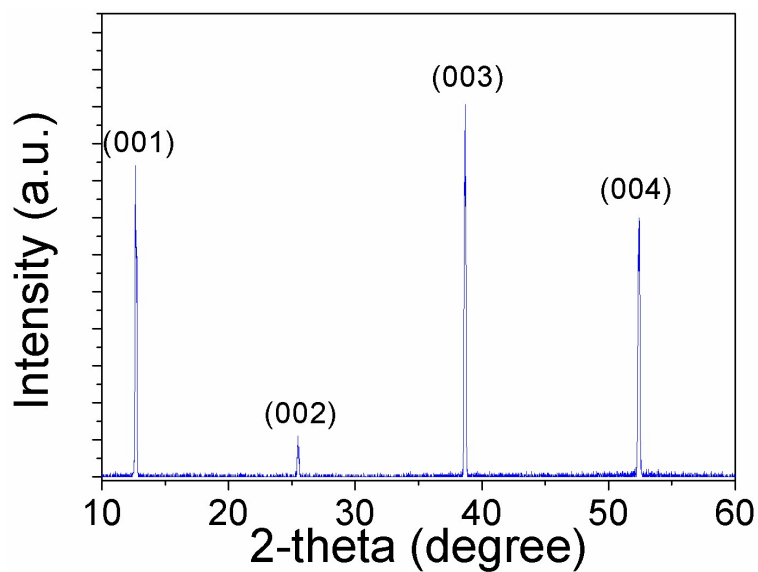
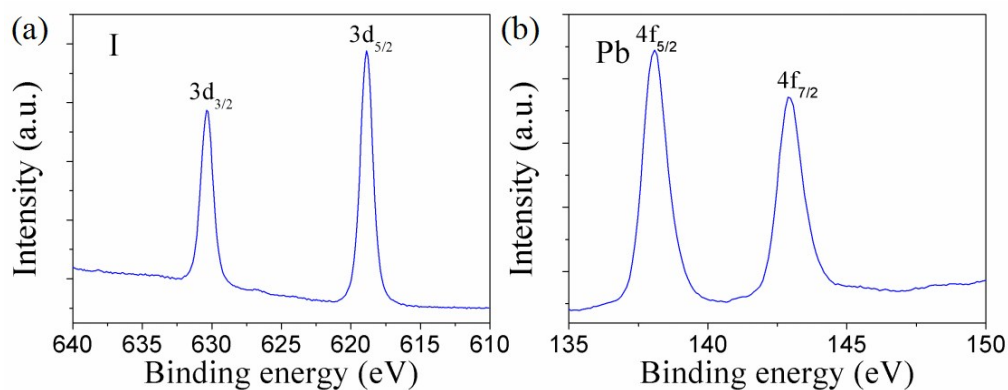**Fig. S5** The X-ray diffraction pattern of bulk PbI_2 crystals.

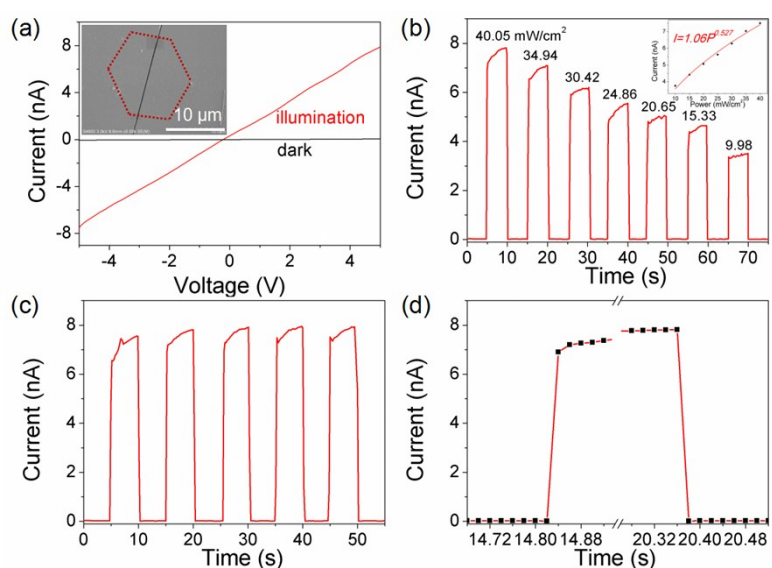**Fig. S6** XPS (a) I 3d and. (b) Pb 4f core-level spectra.

Fig. S7 (a) I-V characteristics of the 9-layer PbI_2 based photodetector under dark and illumination condition. Inset: SEM image of the measured

photodetector. (b) The optoelectronic response properties of this photodetector under irradiation of 450 nm laser with different light power density at a bias voltage of 5 V. Inset: The corresponding light power density dependence of the photocurrent. (c) The photo-switching behaviours, and (d) photocurrent rise and decay time under irradiation of 450 nm laser with a light intensity of 40.05 mW/cm² at the bias voltage of 5 V.
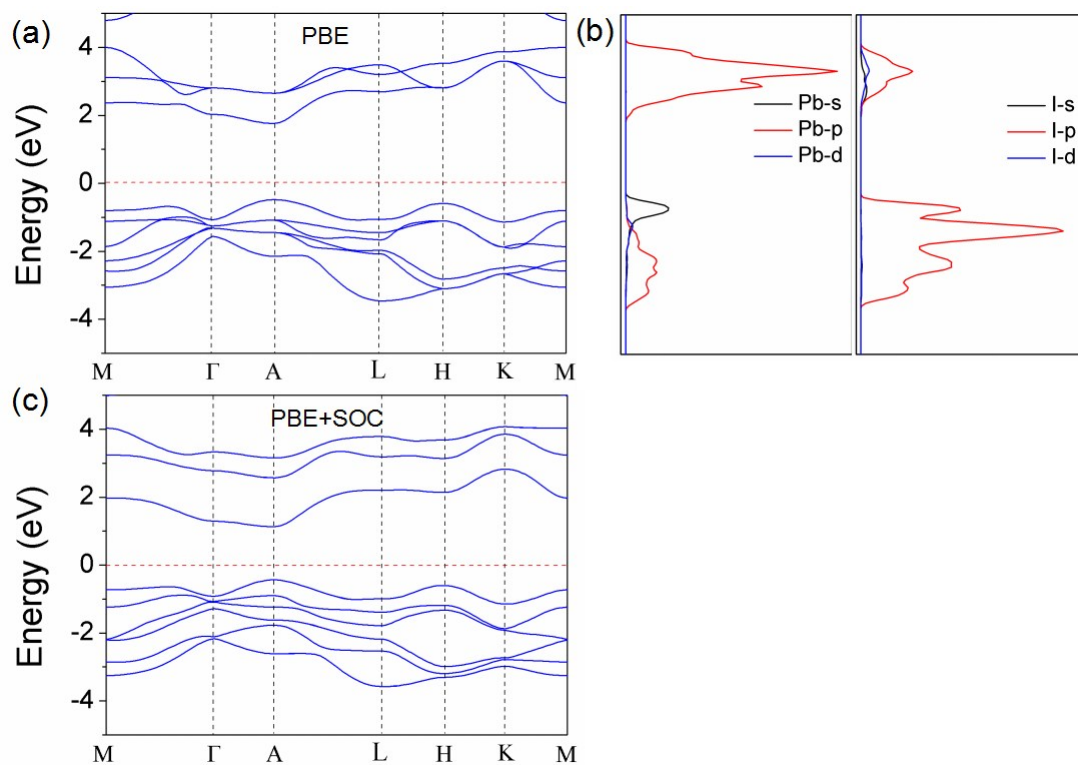

Fig. S8 (a) Electronic band structure of bulk PbI_2 calculated with PBE functional without spin-orbit coupling effect, and (b) the corresponding projected density of states of I and Pb atoms. (c) Electronic band structure of bulk PbI_2 calculated with PBE functional with spin-orbit coupling effect (PBE+SOC).
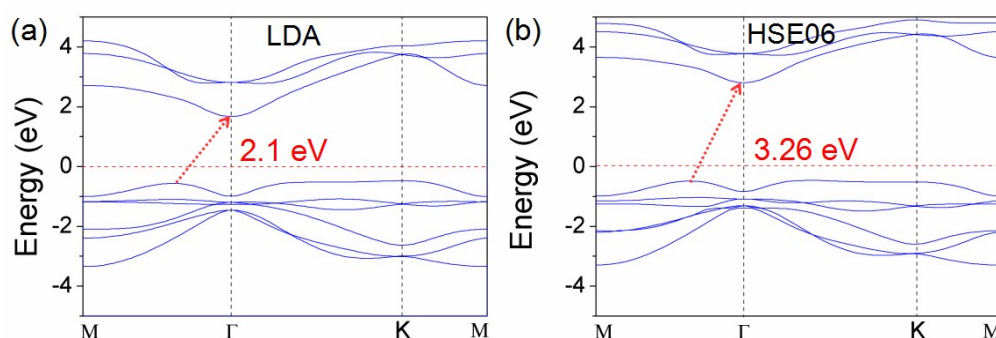

Fig. S9 Electronic band structure of monolayer PbI_2 calculated by LDA (a) and HSE06 (b), respectively.
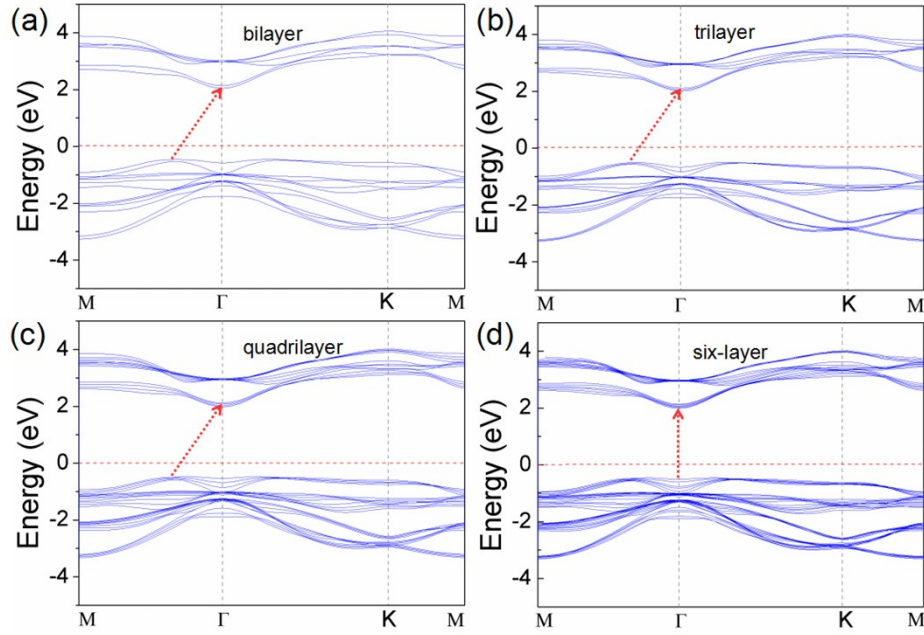
Fig. S10 Calculated band structures of (a) bilayer PbI_2, (b) trilayer PbI_2, (c) quadrilayer PbI_2, and (d) six-layer PbI_2.

Tab. S1 Calculated crystal surface energies (Esurf (J/m^2)) for the low-index surfaces of PbI_2.

	Face						
	(001)	(100)	(010)	(011)	(101)	(110)	(111)
$E_{surf}(J/m^2)$	0.428	4.701	4.701	5.209	4.813	2.640	2.968

References:
1.   P. E. Blöchl, *Phys. Rev. B*, 1994, **50**, 17953.
2.   G. Kresse and J. Furthmüller, *Phys. Rev. B*, 1996, **54**, 11169.
3.   G. Kresse and D. Joubert, *Phys. Rev. B*, 1999, **59**, 1758.
4.   J. P. Perdew, K. Burke and M. Ernzerhof, *Phys. Rev. Lett.*, 1996, **77**, 3865.
5.   J. Klimeš, D. R. Bowler and A. Michaelides, *Phys. Rev. B*, 2011, **83**, 195131.
6.   A. D. Becke, *J. Chem. Phys.*, 1993, **98**, 1372-1377.
7.   J. Heyd, G. E.Scuseria, M. Ernzerhof, *J. Chem. Phys.*, 2003, **118**, 8207−8215.
8.   S. Grimme, *J. Comput. Chem.*, 2006, **27**, 1787-1799.
9.   H. J. Monkhorst and J. D. Pack, *Phys. Rev. B*, 1976, **13**, 5188.
10.   G. Chen, Z. Hou and X. Gong, *Comput. Mater. Sci*, 2008, **44**, 46-52.